Spin-wave modes in ferromagnetic nanodisks, their excitation via alternating currents and fields, and auto-oscillations

D. Mancilla-Almonacid and R. E. Arias
Departamento de Física, CEDENNA, Facultad de Ciencias Físicas y Matemáticas, Universidad de Chile, Av. Blanco Encalada 2008, Santiago, Chile

(Received 7 December 2016; revised manuscript received 17 May 2017; published 28 June 2017)

The excitation of the linear spin wave modes of a soft ferromagnetic free layer of a nanopillar structure through dc-ac currents that traverse the structure is studied, as well as with ac magnetic fields. There is interest in understanding the magnetization dynamics in these structures since they may be used as microwave sources when these nano-oscillators enter into auto-oscillatory regimes. The free layer is a soft ferromagnet, like Permalloy, in the shape of a circular disk, with a very small thickness in the range of the exchange length. Using a description of the magnetization dynamics in terms of a Hamiltonian for weakly interacting waves, we determine the spin wave modes of the structure under two approximations: a very thin film limit, and under a model that includes the effect of the full magnetostatic interaction. We consider direct and parametric excitations of different spin wave modes with ac currents, i.e., with exciting frequency approximately equal to the frequency of the mode or to twice its value, respectively. The Oersted field mainly plays a role in the direct resonant excitation of the modes. Our main conclusion is that for a dc current below the critical value necessary for the development of auto-oscillations, using parametric excitation, a very high value of the ac current is necessary to reach the auto-oscillatory behavior in this geometry. However, if the out-of-plane component of the spin transfer torque is high enough, the ac critical current for auto-oscillations is significantly reduced, leading to a signature for its detection. We comment on parallel pumping and transverse excitation using ac magnetic fields.

DOI: 10.1103/PhysRevB.95.214424

I. INTRODUCTION

Magnetization dynamics at the nanoscale gained an important impetus after the introduction and later experimental verification of the phenomenon of spin transfer torque (STT). In 1996, Slonczewski [1] and Berger [2] simultaneously and independently proposed this effect, which involves the transfer of angular moment from a spin polarized current to a local magnetization, thus affecting its dynamics. This opened the possibility of controlling the magnetization dynamics via STT, and with it came the prospect of new interesting practical devices. Indeed, the areas of spintronics [3–5], i.e., electronics enriched by the spin degree of freedom, and magnonics [6–9], that studies spin waves in natural/artificial materials, were in large part initiated and developed through the introduction of the STT effect.

In this work, we are particularly interested in an application that has emerged from STT, i.e., ferromagnetic nano-oscillators [10–12]. These are localized sources of microwaves that result from nondecaying periodic oscillations of the magnetization at the nanoscale. In some configurations the STT counteracts the effect of dissipation allowing for the magnetization to develop sustained periodic oscillations, or auto-oscillations, that occur at microwave frequencies. These spin transfer nano-oscillators (STNO's) or spin torque nano-oscillators have as basic configuration a "fixed" magnetic layer, a nonmagnetic spacer and a "free" layer. A current runs through these structures that gets spin polarized in the fixed layer, mostly maintains its polarization through the spacer and transfers spin angular momentum to the magnetization of the free layer, thus affecting its dynamics. The magnetization oscillations of the free layer are detected electronically as a voltage signal through the magnetoresistance of these structures (MR). The most common configurations of STNO's are nanopoint contacts, spin valves and magnetic tunnel junctions. Nanocontacts and spin valves use metallic spacers, their difference is in their geometric patterning, nanocontacts have extended layers and the current runs only through a nanocontact, while spin valves correspond to nanopillar structures with restricted and common geometries for the layers. Magnetic tunnel junctions use restricted layer geometries, but the spacers are insulators.

Within ferromagnetic nano-oscillators, we focus our attention on those oscillators in nanopillar structures [13,14], i.e., spin valves, and in their simplest geometry. The latter corresponds to a cylindrical nanopillar with a fixed ferromagnetic layer made of a hard magnetic material separated through a nonmagnetic spacer from a free layer made of a soft ferromagnetic material. We model the free layer as a very thin circular disk, and for the purpose of calculations we use the parameters of Permalloy. A current, with dc-ac components traverses this nanopillar structure, and leads the free layer dynamics.

In a previous work [15], we presented a model, based on a Hamiltonian formulation [16–20] of the dynamics that uses spin wave amplitudes as dynamic variables, with which we studied the dynamics of this free layer under dc currents, in particular instabilities of auto-oscillations associated with the growth of nonuniform modes. Within this model, in this work we studied in detail the effect of adding an ac component to the current density. We were interested in different ways of exciting the linear spin wave normal modes of the disk, and for this we considered two main configurations, i.e., disk magnetized in plane (IP) and out of plane (OP). In particular, we studied the effect of ac currents on the development of auto-oscillations of different normal modes.

In terms of values of the ac excitation frequency, we studied two types of resonant excitations: one that we call direct, in

which the ac frequency is similar to the frequency of a normal mode; and a parametric excitation, in which the ac frequency is approximately twice the frequency of a normal mode. The ac current modifies the dynamic terms associated with the Oersted field and the spin transfer torque, and we take that into account. A conclusion is that the Oersted field is crucial in determining which modes are excited in a direct way. This has been studied in some systems, for example, in Refs. [21–23] the excitation of spin wave modes is studied in a configuration equivalent to the OP, and it is seen that the Oersted field only excites certain modes with specific symmetries, while in Ref. [24] a configuration equivalent to our IP is studied. Also, a main conclusion is that the ac parametric excitation requires very large currents to attain auto-oscillations [25], but this is diminished appreciably if there is an out-of-plane component of the spin transfer torque. The latter means that parametric excitation in a disk geometry may help identify experimentally materials with high out-of-plane components of the spin transfer torque. This may be explained since in our work the out-of-plane component of the spin transfer torque acts like an effective magnetic field in the same direction as the equilibrium magnetization, i.e., it is analogous to the effect of parallel pumping [26,27] and could explain the results obtained in Refs. [28–30]. We also examined the excitation of the spin wave modes of the disk via transverse ac magnetic fields, that compare well with the results of Ref. [31].

In Sec. II, we introduce the model and the Hamiltonian formalism used. In Sec. III, we study the excitation of spin wave normal modes using a simplified model of a disk, i.e., a very thin limit. In Sec. IV, we study the excitation of linear spin wave normal modes using a model that takes into account in its fullness the magnetostatic interaction, i.e., edge effects become important. Finally, in Sec. V, we conclude.

II. MODEL

In the following, we will present a model used to describe the magnetization dynamics of a free layer of a magnetic nanopillar structure. This free layer is made of a soft ferromagnetic material, that in our calculations is taken as Permalloy. In our case, the free layer dynamics is externally influenced by the spin transfer torque induced by a spin polarised electric current (polarised at the fixed layer), and by a magnetic field due to the electric current itself, called the Oersted field.

The geometry of the free layer corresponds to a ferromagnetic disk of circular cross section, of radius R and thickness L, that we consider small. Its magnetization dynamics is described by the Landau-Lifshitz-Slonczewski (LLS) equation, which normalized reads

$$\frac{d\vec{m}}{d\tau} = -\vec{m} \times (\vec{h}_{\text{eff}} + \vec{h}_{\text{stt}}) - \alpha\vec{m} \times [\vec{m} \times (\vec{h}_{\text{eff}} + \vec{h}_{\text{stt}})], \quad (1)$$

with $\vec{m} = \vec{M}/M_s$ the normalized magnetization, M_s the saturation magnetization, $\vec{h}_{\text{eff}} = \vec{H}_{\text{eff}}/4\pi M_s$ the effective field normalized, $\vec{h}_{\text{stt}} = \vec{H}_{\text{stt}}/4\pi M_s$ the effective field associated to spin transfer torque, and α the phenomenological damping constant. Time is normalized as follows, $\tau = |\gamma|4\pi M_s t$, with γ the gyromagnetic ratio of electron. The usual notation for the Landau Lifshitz damping constant is λ, but here we are using α, the Gilbert damping constant, since it is more convenient in

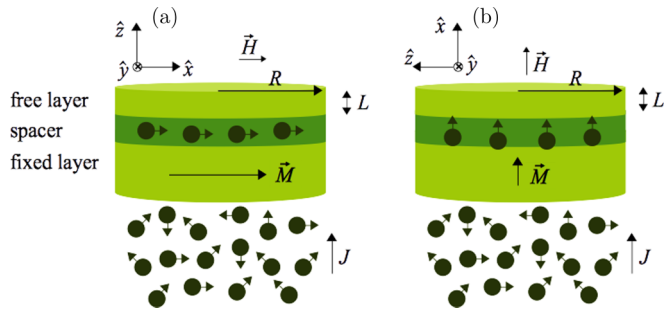

FIG. 1. Configurations of magnetization and spin polarization studied. The circles and arrows represent the electrons and their corresponding spin polarization, respectively. (a) Configuration with the applied magnetic field and spin polarization parallel and in plane (IP). (b) Configuration with the applied magnetic field and spin polarization parallel and perpendicular to the free layer plane (OP). Notice the different choice of Cartesian axes directions in both configurations.

writing Eq. (1) given our choice of time units and normalized magnetization and effective fields (for low dissipation, these constants are related through $\alpha \approx \lambda M_s/|\gamma|$). The expressions for the previously introduced fields are

$$\vec{h}_{\text{eff}} = -\frac{\delta \mathcal{U}_{\text{eff}}}{\delta \vec{m}}, \quad (2a)$$

$$\vec{h}_{\text{stt}} = -\beta_{||} J(\vec{m} \times \hat{p}) - \beta_{\perp} J \hat{p}. \quad (2b)$$

$\mathcal{U}_{\text{eff}}$ is the normalized magnetic free energy

$$\mathcal{U}_{\text{eff}} = \mathcal{U}_Z + \mathcal{U}_D + \mathcal{U}_E, \quad (3)$$

where the different energies considered are: $\mathcal{U}_Z$ is the Zeeman energy associated with the interaction of the magnetization with an applied magnetic field as well as the Oersted field generated by the spin polarized current that traverses the disk, $\mathcal{U}_D$ is the demagnetizing energy, and $\mathcal{U}_E$ is the exchange interaction energy. We do not consider an anisotropy energy, since we consider a soft ferromagnet, as Permalloy. Also, the coefficients associated with the strength of the different terms of the spin transfer effective field of Eq. (2b), i.e., the in-plane coefficient $\beta_{||}$ and the out-of-plane one $\beta_{\perp}$, take the following form [32]:

$$\beta_{||} = \frac{P_{||} h}{(4\pi M_s)^2 e L} \quad \text{and} \quad \beta_{\perp} = \frac{P_{\perp} h}{(4\pi M_s)^2 e L}, \quad (4)$$

with $P_{||}$ and $P_{\perp}$ the polarization factors, h Planck's constant, and e the magnitude of an electron charge. The applied current density is J, and the direction of spin polarization of the electric current is $\hat{p}$. The parameter $\beta_{\perp}$ is larger in the case that the spacer between the fixed and free layers of the nanopillar structure is an insulating material, while for a metallic spacer it should be negligible [33,34].

We consider two configurations under which the magnetization dynamics of the disk is studied, Fig. 1 represents both of them. In Fig. 1(a), both the applied magnetic field and the spin polarization are in plane, and in the same direction (IP configuration). In Fig. 1(b), both the applied magnetic field and the spin polarization are perpendicular to the free layer plane, in the same direction (OP configuration). In both cases,

the Cartesian axis are taken such that the spin polarization is $\hat{p} = \hat{x}$.

Since the LLS equation for the magnetization dynamics conserves the magnitude of the magnetization ($|\vec{m}^2| = 1$), the three components of the magnetization are not independent, and only two of them are necessary to describe the dynamics. Due to this and since we are interested in a linear dynamics close to the equilibrium magnetization that is almost saturated ($\vec{m}^{\rm eq} \approx m_x\hat{x}$) in both configurations, it is convenient to introduce through the classical Holstein-Primakoff transformation the complex variables $a(\vec{\rho},\tau)$, $a^*(\vec{\rho},\tau)$ in order to describe the magnetization dynamics:

$$\left.\begin{aligned} m_x &= 1 - aa^* \\ m_y = (a - a^*)\sqrt{2 - aa^*}/(2i) \\ m_z = (a + a^*)\sqrt{2 - aa^*}/2 \end{aligned}\right\} \Leftrightarrow a = \frac{im_y + m_z}{\sqrt{1 + m_x}}. \quad (5)$$

Thus a and a^* represent a perturbation of the initial equilibrium state, and are the classical analogs of the quantum-mechanical operators of creation and annihilation of magnons. The LLS equation [Eq. (1)] for the magnetization dynamics is transformed to the following equations in a and a^*:

$$i\frac{da}{d\tau} \approx (1 - i\alpha)\frac{\delta \mathcal{U}_t}{\delta a^*}, \quad (6a)$$

$$i\frac{da^*}{d\tau} \approx -(1 + i\alpha)\frac{\delta \mathcal{U}_t^*}{\delta a}, \quad (6b)$$

where an effective complex free energy $\mathcal{U}_t = \mathcal{U}_{\rm eff} + i\mathcal{U}_{\rm stt}$ was introduced, whose real part is the conservative part associated with the Zeeman, demagnetizing and exchange fields, and whose imaginary part is associated with the spin transfer torque. These free energies just presented have been normalized, i.e., $\mathcal{U} = E/(4\pi M_s^2)$, with E representing full free energies. An approximate sign was introduced in Eqs. (6a) and (6b) since the dissipative term in the equation of motion was taken in its linear approximation.

In our model we consider that the thickness of the disk is of the order of the exchange length, i.e., in the order of nanometers, and thus we assume that the magnetization is uniform over the thickness, i.e., $a = a(\vec{\rho},\tau)$, with $\vec{\rho}$ an in-plane vector. In order to describe the dynamics in variables appropriate to the geometry of the disk, we introduce a change of variables from the field $a(\vec{\rho},\tau)$ to amplitudes $a_{mj}(\tau)$, that are the coefficients of an expansion of $a(\vec{\rho},\tau)$ in a complete basis in two dimensions:

$$a(\vec{\rho},\tau) = N_{00}a_{00}(\tau) + \sum_{m=-\infty}^{\infty}\sum_{j=1}^{\infty} N_{mj}a_{mj}(\tau)J_m(\chi_{mj}\rho/R)e^{im\phi}, \quad (7)$$

with ρ and ϕ polar coordinates with origin in the center of the disk. The previous basis, that involves Bessel functions in the radial coordinate and sinusoidal periodic functions in the azimuthal angle, uses functions that have zero slope at the edge of the disk since we consider a free boundary condition there, i.e., that the surface anisotropy is negligible, or $\partial\vec{m}/\partial\rho|_{\rho=R}=0$. This implies that the coefficients χ_{mj} appearing in the expansion of Eq. (7) are zeros of the first derivatives of the Bessel functions, i.e., $J'_m(\chi_{mj}) = 0$. We did not include dipolar pinning [35,36] explicitly in our calculations, since this type of pinning should come out naturally from our calculations in which we consider the full magnetostatic interaction and the associated magnetostatic boundary conditions. The basis set satisfies the following orthogonality relation:

$$\int dV J_m(\chi_{mj}\rho/R)J_{m'}(\chi_{m'j'}\rho/R)e^{i(m+m')\phi} = (-1)^m\delta^m_{-m'}\delta^j_{j'}/N^2_{mj} \quad (8)$$

and thus

$$a_{mj}(\tau) = N_{mj}\int dV a(\vec{\rho},\tau)J_m(\chi_{mj}\rho/R)e^{-im\phi}. \quad (9)$$

The transformation of variables from a to a_{mj} is canonical, i.e.,

$$\frac{\partial a}{\partial a_{mj}} = \frac{\delta a^*_{mj}}{\delta a^*}, \quad (10)$$

if the coefficients N_{mj} satisfy

$$N_{00} = 1/\sqrt{V}, \quad (11a)$$

$$N_{mj} = 1/\sqrt{-J_m(\chi_{mj})J''_m(\chi_{mj})V}, \quad (11b)$$

with $V = \pi R^2 L$ the volume of the free layer. Since the transformation is canonical, the equations of motion in the new variables a_{mj} take the simple form

$$i\frac{da_{mj}}{d\tau} \approx (1 - i\alpha)\frac{\partial \mathcal{U}_t}{\partial a^*_{mj}}, \quad (12a)$$

$$i\frac{da^*_{mj}}{d\tau} \approx -(1 + i\alpha)\frac{\partial \mathcal{U}_t^*}{\partial a_{mj}}. \quad (12b)$$

In the following, we describe the different terms of the free energy. In the case of an equilibrium magnetization configuration that is nonuniform, terms of the free energy that are higher order than two in the a_{mj} variables are required in order to properly describe the magnetization dynamics—those are presented in detail in Appendix.

The Zeeman energy of interaction with a magnetic field applied in direction x is given exactly by

$$\mathcal{U}_Z = h_x\int aa^*dV = h_x\sum_{mj} a_{mj}a^*_{mj}, \quad (13)$$

with $h_x = H_x/(4\pi M_s)$ a normalized magnetic field applied along the x direction.

One may also consider the interaction with the magnetic field produced by the electric current running through the disk, or the Oersted field, which is given by Ampere's law

$$\oint \vec{H}\cdot d\vec{l} = \frac{4\pi}{c}\int \vec{J}\cdot d\vec{S}. \quad (14)$$

We approximate that the current density running through the disk is uniform over its section, leading to the following expression for the Oersted field:

$$\vec{H}_O = \frac{2\pi J\rho}{c}\hat{\phi}. \quad (15)$$

Thus the Zeeman energy density of interaction with the Oersted field takes the form

$$\mathcal{W}_O = -\vec{H}_O \cdot \vec{M} = -\frac{2\pi M_s J\rho}{c} m_\phi. \tag{16}$$

In the in-plane configuration (IP), $m_\phi = -m_x \sin\phi + m_y \cos\phi$, leading to the following approximate energy of interaction with the Oersted field:

$$\mathcal{U}_O^{IP} \approx h_O \int \left[-aa^* \sin\phi + \frac{a^* - a}{\sqrt{2}i} \times \left(1 - \frac{aa^*}{4}\right) \cos\phi \right] \frac{\rho}{R} dV, \tag{17}$$

with $h_O = |\vec{H}_O(\rho = R)|/(4\pi M_s) = JR/(2M_s c)$, i.e., a normalized magnitude of the Oersted field at the edge of the disk. To the first order, the previous Oersted interaction energy is approximately

$$\mathcal{U}_O^{IP(1)} = -iV \frac{h_O}{\sqrt{2}} \sum_j (a_{-1j} + a_{1j}^* - \text{c.c.}) i_j^O, \tag{18}$$

where $i_j^O = N_{1j} J_2(\chi_{1j})/\chi_{1j}$. Expressions of higher orders of the Oersted interaction energy are given in Appendix A 1. In the out-of-plane configuration, $m_\phi = -m_z \sin\phi + m_y \cos\phi$, which leads to

$$\mathcal{U}_O^{OP} \approx i h_O \int [(ae^{-i\phi} - a^* e^{i\phi})(1 - aa^*/4)/\sqrt{2}] \frac{\rho}{R} dV. \tag{19}$$

To the first order, the previous Oersted interaction energy is approximately

$$\mathcal{U}_O^{OP(1)} \approx i h_O \sqrt{2} V \sum_j (a_{1j} - a_{1j}^*) i_j^O, \tag{20}$$

with $i_j^O = N_{1j} J_2(\chi_{1j})/\chi_{1j}$. Higher-order terms are presented in Appendix A 2.

Also, the exchange energy density is given by

$$\mathcal{W}_E = A[(\vec{\nabla} m_x)^2 + (\vec{\nabla} m_y)^2 + (\vec{\nabla} m_z)^2], \tag{21}$$

where A is the exchange constant, and to fourth order the exchange energy takes the form

$$\mathcal{U}_E \approx h_E \int \left[\vec{\nabla} a \cdot \vec{\nabla} a^* + \frac{1}{4} a^2 (\vec{\nabla} a^*)^2 + \frac{1}{4} a^{*2} (\vec{\nabla} a)^2 \right] R^2 dV, \tag{22}$$

with $h_E = A/(2\pi M_s^2 R^2) = (l_E/R)^2$, l_E is the exchange length (approximately 6 nm in permalloy). To second order, the exchange energy is given by

$$\mathcal{U}_E^{(2)} = \sum_{mj} h_E^{mj} a_{mj} a_{mj}^*, \tag{23}$$

with $h_E^{mj} \equiv h_E \chi_{mj}^2$. Higher-order terms of the exchange energy are given in Appendix B (in our more complete version of the model, the equilibrium configuration is quasiuniform, thus we need higher order terms of the free energy in order to determine the linear spin wave modes with respect to this configuration).

With respect to the demagnetizing energy, we present a simplified model of the disk where we approximate the demagnetizing field by its very thin film limit, i.e., its only component is along the direction perpendicular to the plane of the film $H_D = -4\pi M_\perp$ and $\mathcal{U}_D = 2\pi M_\perp^2 V$, and also a model of the disk where the demagnetizing field is taken in its full form, with details found in Appendix C.

The expression of the effective energy associated with the spin transfer torque is given by

$$\mathcal{U}_{\text{stt}} = \beta_{||} J \int aa^*(1 - aa^*/4) dV + i\beta_\perp J \int aa^* dV. \tag{24}$$

The second-order terms of the previous effective energy are given by

$$\mathcal{U}_{stt}^{(2)} = (\beta_{||} + i\beta_\perp) J \sum_{mj} a_{mj} a_{mj}^*, \tag{25}$$

with fourth-order terms shown in Appendix D.

III. EXCITATION OF SPIN WAVE MODES OF THE DISK, SIMPLE MODEL

We start our study of the excitation of the spin wave modes of a disk, considering a simple model of it: we assume a very thin limit, with the ratio of the thickness of the film over its radius as very small, i.e., $L/R \ll 1$. In this case the demagnetizing field may be approximated as $\vec{H}_D = -4\pi M_z \hat{z}$ in the in-plane configuration (IP), and as $\vec{H}_D = -4\pi M_x \hat{x}$ in the out-of-plane configuration (OP). Within this simplified model, in both cases the equilibrium magnetization corresponds to a completely saturated state in the direction of the applied field, i.e., in the $\hat{x}$ axis (in the OP configuration a magnetic field perpendicular to the plane needs to be applied with magnitude greater than $4\pi M_s$). We will study the excitation of magnetization dynamics through the injection of a spin polarised current in the following.

In all the calculations that will be presented in this work, we considered that the free layer is made of Permalloy, a soft ferromagnet with the following associated parameters: saturation magnetization $M_s = 800$ emu cm^{-3}, exchange constant $A = 1.3 \times 10^{-6}$ erg cm^{-1} and exchange length $l_E = 5.7$ nm. Also, we consider that the radius of the disk is given by $R = 50$ nm, the thickness $L = 5$ nm, and the phenomenological dissipation constant $\alpha = 0.01$. We consider that the parameter associated with spin transfer torque parallel to the plane is $P_{||} = 0.17$, and that perpendicularly to the plane $P_\perp$ is considered variable.

A. In-plane configuration (IP)

Under our simple model of a disk, the demagnetizing energy in the in-plane configuration (IP) takes the form

$$\mathcal{U}_D = \frac{1}{4} \int (a + a^*)^2 dV = \frac{1}{4} \sum_{mj} |(a_{mj} + (-1)^m a_{-mj}^*)|^2. \tag{26}$$

The equations of motion that follow from Eqs. (12a), (12b), (13), (23), (25), and (26) if there is an applied dc current density $J = J_{\text{dc}}$, are given by

$$i \frac{d}{d\tau} \begin{pmatrix} a_{mj} \\ a_{-mj}^* \end{pmatrix} = \begin{pmatrix} A_{mj} & (-1)^m B_{mj} \\ -(-1)^m B_{mj}^* & -A_{mj}^* \end{pmatrix} \begin{pmatrix} a_{mj} \\ a_{-mj}^* \end{pmatrix}, \tag{27}$$

with $A_{mj} \equiv (1-i\alpha)[(h_x + 1/2 + h_E^{mj}) + (i\beta_{||} - \beta_\perp)J_{\rm dc}]$ and $B_{mj} \equiv (1-i\alpha)/2$. In order to solve these equations and diagonalize the problem, we do the following Bogoliubov transformation:

$$\begin{pmatrix} a_{mj} \\ a^*_{-mj} \end{pmatrix} = \begin{pmatrix} \lambda_{mj} & -(-1)^m \mu_{mj} \\ -(-1)^m \mu^*_{mj} & \lambda^*_{mj} \end{pmatrix} \begin{pmatrix} b^{(1)}_{mj} \\ b^{(2)}_{mj} \end{pmatrix}, \quad (28)$$

with

$$\lambda_{mj} = \sqrt{\frac{Re(A_{mj}) + \omega_{mj}}{2\omega_{mj}}}, \quad (29a)$$

$$\mu_{mj} = \sqrt{\frac{Re(A_{mj}) - \omega_{mj}}{2\omega_{mj}}}\sqrt{\frac{B_{mj}}{B^*_{mj}}}, \quad (29b)$$

and

$$\omega_{mj} = \sqrt{[Re(A_{mj})]^2 - |B_{mj}|^2} = \sqrt{\left(h_x + h_E^{mj} + 1/2 + (\alpha\beta_{||} - \beta_\perp)J_{dc}\right)^2 - (1+\alpha^2)/4}. \quad (30)$$

The new equation of motion for the variables $b^{(1)}_{mj}$ and $b^{(2)}_{mj}$ becomes

$$i\frac{d}{d\tau}\begin{pmatrix} b^{(1)}_{mj} \\ b^{(2)}_{mj} \end{pmatrix} = \begin{pmatrix} \omega_{mj} + i\gamma_{mj} & 0 \\ 0 & -\omega_{mj} + i\gamma_{mj} \end{pmatrix} \begin{pmatrix} b^{(1)}_{mj} \\ b^{(2)}_{mj} \end{pmatrix}, \quad (31)$$

with their direct solutions $b^{(1)}_{mj}(\tau) = b^{0(1)}_{mj} e^{(-i\omega_{mj} + \gamma_{mj})\tau}$ and $b^{(2)}_{mj}(\tau) = b^{0(2)}_{mj} e^{(i\omega_{mj} + \gamma_{mj})\tau}$. These represent the normal modes of the system that oscillate at frequency ω_{mj} (a normalized frequency, indeed $f_{mj} = 2M_s|\gamma|\omega_{mj}$ is the frequency in hertz), and that include their effective dissipation constant

$$\gamma_{mj} = {\rm Im}(A_{mj}) = \beta_{||} J_{\rm dc} - \alpha\left(h_x + h_E^{mj} + 1/2 - \beta_\perp J_{\rm dc}\right). \quad (32)$$

In order for the mj mode to grow exponentially and to observe auto-oscillations of the magnetization, it should happen that $\gamma_{mj} > 0 \Rightarrow J_{\rm dc} > J^C_{\rm dc} = \alpha(h_x + h_E^{mj} + 1/2)/(\beta_{||} + \alpha\beta_\perp)$, i.e., $J^C_{\rm dc}$ is a critical dc current.

We now consider the application of an alternating current, with a dc current lower than the critical current, i.e., $J = J_{\rm dc} + J_{\rm ac}\cos(\Omega\tau)$ with $J_{\rm dc} < J^C_{\rm dc}$. Since applying an ac current to the structure is technically simple, it is interesting to explore its effect in the magnetization dynamics as a means to understand it and eventually control it in a desired way. The ac current has an associated ac Oersted field, but it also introduces naturally a parametric excitation of the system since the spin transfer torque term is proportional to the current, thus we focused on understanding both effects. In particular, in the case of parametric excitation, we consider that the dc current is below its critical value (if not, one needs to do a nonlinear analysis of the problem, due to a large excitation of the system, which was not the goal here) and we focus on the initiation of auto-oscillations; indeed, we look for magnetization oscillations that are synchronized with half the frequency of the ac current, i.e., $\Omega/2$. The equations of motion for the pair (a_{mj}, a^*_{-mj}) then take the form

$$i\frac{d}{d\tau}\begin{pmatrix} a_{mj} \\ a^*_{-mj} \end{pmatrix} = \begin{pmatrix} A_{mj} & (-1)^m B_{mj} \\ -(-1)^m B^*_{mj} & -A^*_{mj} \end{pmatrix} \begin{pmatrix} a_{mj} \\ a^*_{-mj} \end{pmatrix} + J_{\rm ac}\cos(\Omega\tau)\left[\begin{pmatrix} D_{mj} \\ -D^*_{mj} \end{pmatrix} + \begin{pmatrix} C_{mj} & 0 \\ 0 & -C^*_{mj} \end{pmatrix}\begin{pmatrix} a_{mj} \\ a^*_{-mj} \end{pmatrix}\right], \quad (33)$$

with $C_{mj} \equiv (1-i\alpha)(i\beta_{||} - \beta_\perp)$ and $D_{mj} \equiv (1-i\alpha) i V R(\delta^m_{-1} - \delta^m_1) i^O_j/(2\sqrt{2}M_s c)$. Using the same change of variables of Eq. (28), we obtain

$$i\frac{d}{d\tau}\begin{pmatrix} b^{(1)}_{mj} \\ b^{(2)}_{mj} \end{pmatrix} = \begin{pmatrix} \omega_{mj} + i\gamma_{mj} & 0 \\ 0 & -\omega_{mj} + i\gamma_{mj} \end{pmatrix} \begin{pmatrix} b^{(1)}_{mj} \\ b^{(2)}_{mj} \end{pmatrix} + J_{\rm ac}\cos(\Omega\tau)\begin{pmatrix} \lambda^*_{mj} D_{mj} - (-1)^m \mu_{mj} D^*_{mj} \\ -\lambda_{mj} D^*_{mj} + (-1)^m \mu^*_{mj} D_{mj} \end{pmatrix}$$
$$+ J_{\rm ac}\cos(\Omega\tau)\begin{pmatrix} Re(A_{mj})Re(C_{mj})/\omega_{mj} + iIm(C_{mj}) & -(-1)^m B_{mj} Re(C_{mj})/\omega_{mj} \\ (-1)^m B^*_{mj} Re(C_{mj})/\omega_{mj} & -Re(A_{mj})Re(C_{mj})/\omega_{mj} + iIm(C_{mj}) \end{pmatrix}\begin{pmatrix} b^{(1)}_{mj} \\ b^{(2)}_{mj} \end{pmatrix}. \quad (34)$$

If the frequency of the alternating current is $\Omega \sim \omega_{mj}$, a response at the same frequency is expected. Thus we propose solutions of the type $b^{(1)}_{mj} = b^{0(1)}_{mj} e^{-i\Omega\tau}$ and $b^{(2)}_{mj} = b^{0(2)}_{mj} e^{i\Omega\tau}$ to Eq. (34), and considering only resonant terms this equation becomes approximately

$$\begin{pmatrix} \omega_{mj} - \Omega + i\gamma_{mj} & 0 \\ 0 & -\omega_{mj} + \Omega + i\gamma_{mj} \end{pmatrix}\begin{pmatrix} b^{0(1)}_{mj} \\ b^{0(2)}_{mj} \end{pmatrix} = -\frac{J_{\rm ac}}{2}\begin{pmatrix} \lambda^*_{mj} D_{mj} - (-1)^m \mu_{mj} D^*_{mj} \\ -\lambda_{mj} D^*_{mj} + (-1)^m \mu^*_{mj} D_{mj} \end{pmatrix}. \quad (35)$$

Since $D_{mj} \sim (\delta^m_{-1} - \delta^m_1)$, the modes excited by the Oersted field are those with indices $m = \pm 1$, they correspond to degenerate modes, with one circulating in clockwise sense and the other counterclockwise. One of them ($m = 1$) is plotted in Fig. 2.

If we consider excitations of the spin wave normal modes through an applied ac magnetic field perpendicular to the equilibrium magnetization (transverse pumping), with $h_y = h_{\rm ap}\cos(\Omega\tau)$, one obtains $D_{mj} \sim \delta^m_0 \delta^j_0$, meaning that only the uniform mode would be excited with this mechanism [31].

Now if we consider that the frequency of the alternating current is $\Omega \sim 2\omega_{mj}$, i.e., under parametric resonance conditions, the response to the excitation is expected at half of this frequency. Thus we search for solutions of the form $b^{(1)}_{mj} = b^{0(1)}_{mj} e^{(-i\Omega/2 + \Gamma_{mj})t}$ and $b^{(2)}_{mj} = b^{0(2)}_{mj} e^{(i\Omega/2 + \Gamma_{mj})t}$ to Eq. (34), and when only resonant terms are considered, this equation

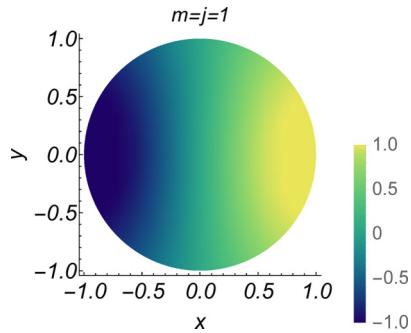

FIG. 2. Spatial form of the first $m = 1$ modes excited by the Oersted field in the IP configuration. The component $m_z \approx 2\mathrm{Re}(a)$ of the magnetization is plotted for an applied magnetic field $h_x = 0.1$ (normalized by $4\pi M_s$). One circulates in clockwise sense and the other counterclockwise.

becomes

$$\begin{pmatrix} \left(\frac{\Omega}{2} - \omega_{mj}\right) + i(\Gamma_{mj} - \gamma_{mj}) & \frac{(-1)^m(\alpha\beta_{||} - \beta_\perp)B_{mj}J_{\mathrm{ac}}}{2\omega_{mj}} \\ \frac{(-1)^m(\beta_\perp - \alpha\beta_{||})B^*_{mj}J_{\mathrm{ac}}}{2\omega_{mj}} & \left(\omega_{mj} - \frac{\Omega}{2}\right) + i(\Gamma_{mj} - \gamma_{mj}) \end{pmatrix} \times \begin{pmatrix} b^{0(1)}_{mj} \\ b^{0(2)}_{mj} \end{pmatrix} = 0. \tag{36}$$

The solution to Eq. (36) is obtained imposing the determinant of the matrix involved to be null, i.e.,

$$\left(\frac{(\alpha\beta_{||} - \beta_\perp)J_{\mathrm{ac}}}{2\omega_{mj}}\right)^2 |B_{mj}|^2 = (\Gamma_{mj} - \gamma_{mj})^2 + \left(\frac{\Omega}{2} - \omega_{mj}\right)^2. \tag{37}$$

The solutions found, i.e., $b^{(1)}_{mj} = b^{0(1)}_{mj} e^{(-i\Omega/2+\Gamma_{mj})t}$ and $b^{(2)}_{mj} = b^{0(2)}_{mj} e^{(i\Omega/2+\Gamma_{mj})t}$ start growing exponentially if $\Gamma_{mj} > 0$, thus the critical ac current for instability corresponds to $\Gamma_{mj} = 0$, or

$$J^C_{\mathrm{ac}} = \frac{2\omega_{mj}}{|\alpha\beta_{||} - \beta_\perp|}\sqrt{\frac{\gamma^2_{mj} + (\Omega/2 - \omega_{mj})^2}{|B_{mj}|^2}}. \tag{38}$$

This critical ac current density is minimal when the frequency of the alternating current is the double of the natural frequency of the oscillating mode ($\Omega = 2\omega_{mj}$), i.e.,

$$J^C_{\mathrm{ac}}(\Omega = 2\omega_{mj}) = \frac{2\omega_{mj}|\gamma_{mj}|}{|\alpha\beta_{||} - \beta_\perp||B_{mj}|}. \tag{39}$$

This expression for this critical alternating current density depends on the dc current applied, and it is plotted in Fig. 3 for the uniform mode ($m = j = 0$), considering an applied magnetic field $h_x = 0.1$. It is observed that this critical ac current is very high, and that the presence of an out-of-plane component of the spin transfer torque may diminish considerably the value of this critical ac current density, and in this way it may become practical to excite parametrically the uniform mode.

If one were to plot J_{ac} versus J_{dc} for nonuniform modes the corresponding magnitude of the slope would be larger than in Fig. 3. Thus, to excite a nonuniform mode into auto-oscillation, one needs a higher ac current than for the uniform mode.

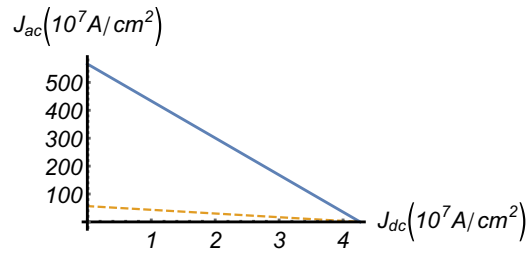

FIG. 3. Critical alternating current density $J^C_{\mathrm{ac}}(\Omega = 2\omega_{00})$ necessary to induce auto-oscillations of the macrospin, as a function of the dc current density traversing the disk, with an applied magnetic field $h_x = 0.1$ (normalized by $4\pi M_s$), IP configuration. The blue line corresponds to $\beta_\perp = 0$, while the orange to $\beta_\perp = 0.1\beta_{||}$.

B. Out-of-plane configuration (OP)

In the OP configuration, and within the simple model of the demagnetizing field, the normalized demagnetizing energy takes the form $\mathcal{U}_D = m_x^2/2 = (1 - aa^*)^2$, meaning that to quadratic order (neglecting constant terms) it takes the form $\mathcal{U}_D = -aa^* = -\sum_{m,j} a_{mj}a^*_{mj}$. Following Eq. (12a), the dynamic equation for the complex variable a_{mj} to linear order, and considering dissipation and the spin transfer torque, at a given applied dc current density $J = J_{\mathrm{dc}}$, is given by

$$i\frac{da_{mj}}{d\tau} = (1 - i\alpha)\left[h_x - 1 + h^E_{mj} + (i\beta_{||} - \beta_\perp)J_{\mathrm{dc}}\right]a_{mj}, \tag{40}$$

whose solution is simply $a_{mj}(\tau) = a^0_{mj}e^{(-i\omega_{mj}+\gamma_{mj})\tau}$, with

$$\omega_{mj} = h_x - 1 + h^{mj}_E - \beta_\perp J_{\mathrm{dc}} + \alpha\beta_{||}J_{\mathrm{dc}}, \tag{41}$$

$$\gamma_{mj} = \beta_{||}J_{\mathrm{dc}} - \alpha\left(h_x - 1 + h^{mj}_E - \beta_\perp J_{\mathrm{dc}}\right). \tag{42}$$

Thus one finds the frequency ω_{mj} of a normal mode, and its effective growth/decay constant γ_{mj}. This becomes an auto-oscillatory solution if the dc current density exceeds a critical value J^C_{dc} such that $\gamma_{mj} = 0$, i.e., $J^C_{\mathrm{dc}} = \alpha(h_x - 1 + h^{mj}_E)/(\beta_{||} + \alpha\beta_\perp)$. If one adds an alternating current density, i.e., $J = J_{\mathrm{dc}} + J_{\mathrm{ac}}\cos(\Omega\tau)$ and considers the effect of the Oersted field, the equation of motion for a_{mj} is modified to

$$\begin{aligned} i\frac{da_{mj}}{d\tau} =& (1 - i\alpha)\left[h_x - 1 + h^{mj}_E + (i\beta_{||} - \beta_\perp)J_{\mathrm{dc}}\right]a_{mj} \\ &+ (1 - i\alpha)(i\beta_{||} - \beta_\perp)J_{\mathrm{ac}}\cos(\Omega\tau)a_{mj} \\ &+ (1 - i\alpha)E_{mj}J_{\mathrm{ac}}\cos(\Omega\tau), \end{aligned} \tag{43}$$

with $E_{mj} = -i\sqrt{2}VR\delta^m_1 i^O_j/(2M_s c)$ [from Eqs. (12a) and (20)]. Thus the modes (m, j) cannot be excited parametrically. Also, the modes that are excited directly by the Oersted field, correspond to $m = 1$. The first corresponds to the mode $m = j = 1$, with $m_z \approx \sqrt{2}Re(a)$, as follows:

$$m_z = \sqrt{2}N_{11}a^0_{11}J_1(\chi_{11}\rho/R)\cos(\phi - \omega_{11}t), \tag{44}$$

which corresponds to a mode rotating anticlockwise, and is represented in the following Fig. 4. As for the IP configuration, if the spin wave normal modes are excited via an ac magnetic field perpendicular to the equilibrium magnetization, with

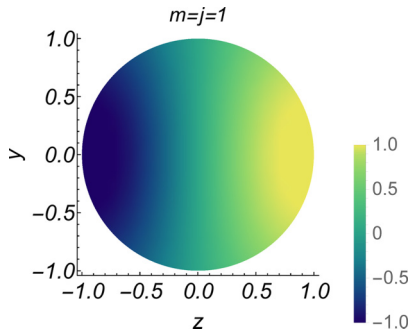

FIG. 4. Spatial form of the first mode excited by the Oersted field in the configuration OP. The component $m_z \approx 2\mathrm{Re}(a)$ of the magnetization is plotted at an applied magnetic field $h_x = 1.1$ (normalized by $4\pi M_s$). The mode gyrates counter-clockwise.

$h_y = h_{\mathrm{ap}} \cos(\Omega\tau)$, we obtain $E_{mj} \sim \delta_0^m \delta_0^j$, so that only the uniform mode would be excited by this mechanism.

IV. EXCITATION OF SPIN WAVE MODES OF THE DISK, MODEL WITH FULL DEMAGNETIZING FIELD

In the following, we study the dynamics of the magnetization of the disk using a model that takes into account the full demagnetizing effects. In particular, the effect of the edges of the disk will be relevant in this approximation. In order to determine the spin wave modes of the disk and their excitation, it is necessary to determine first the equilibrium magnetization configuration, as is done in the following.

A. Equilibrium configuration

If a dc current density $J = J_{\mathrm{dc}}$ is applied, and is lower than the critical current density necessary to observe auto-oscillations of the magnetization, the equilibrium configuration corresponds to one that satisfies

$$\left.\frac{\partial \mathcal{U}_t^{\mathrm{dc}}}{\partial a_{mj}^*}\right|_{\mathrm{eq}} = 0, \tag{45}$$

where $\mathcal{U}_t^{\mathrm{dc}} = \mathcal{U}_Z + \mathcal{U}_D + \mathcal{U}_E + \mathcal{U}_O^{\mathrm{dc}} + i\mathcal{U}_{\mathrm{stt}}^{\mathrm{dc}}$, i.e., the different terms correspond to the applied magnetic field, the demagnetizing field, the exchange field, the Oersted field and the spin transfer torque, respectively. Thus the equilibrium configuration will depend on the strength of the applied magnetic field and the dc current density. The critical current densities are $J_{\mathrm{dc}}^C \approx 3.44 \times 10^7\ \mathrm{A\,cm^{-2}}$ and $J_{\mathrm{dc}}^C \approx 1.88 \times 10^7\ \mathrm{A\,cm^{-2}}$ for the IP and OP configurations respectively, for our disk of permalloy of radius $R = 50$ nm, and thickness $L = 5$ nm. The system of nonlinear equations that determine the equilibrium configurations was solved by an iterative method, that is an extension of the Newton-Raphson method. Initially, one obtains an approximate solution via the linear version of the equations, and this becomes the initial solution of an iterative process that converges to the nonlinear solution.

In Fig. 5, two states of equilibrium are represented for the configurations IP and OP: in both cases, the dc current is lower than the respective threshold to initiate auto-oscillations of the magnetization. Figure 5(a) represents the equilibrium

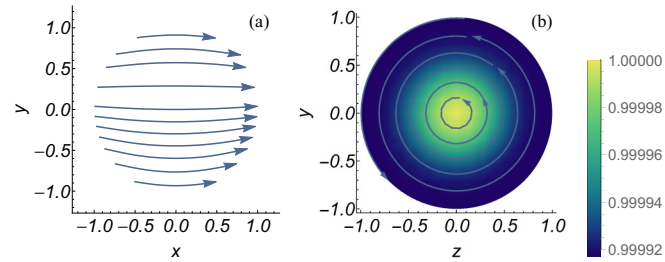

FIG. 5. Equilibrium magnetization for two configurations. (a) IP configuration: we consider an applied field $h_x = 0.1$ and a current density applied $J_{\mathrm{dc}} = 3 \times 10^7\ \mathrm{A\,cm^{-2}}$. The magnetization is in plane ($m_z = 0$). (b) OP configuration: we consider an applied field $h_x = 1.1$ and an applied current density $J_{\mathrm{dc}} = 1.5 \times 10^7\ \mathrm{A\,cm^{-2}}$. The color scale represents the magnetization component m_x, and the vectors the rotating in-plane components of the magnetization.

magnetization in the IP configuration for an in of plane applied magnetic field $h_x = 0.1$, a_{mj}^{eq} is real if m is even and a_{mj}^{eq} is imaginary if m is odd. One has that $a_{-mj}^{\mathrm{eq}} = -a_{mj}^{\mathrm{eq}}$, so that $m_z = 0$, i.e., the magnetization is in the plane of the disk. In absence of an applied current, the magnetization is symmetric with respect to the $y = 0$ axis. This symmetry is broken by a dc current due to the effect of the associated Oersted field. In Fig. 5(b), the OP equilibrium magnetization is presented for an out-of-plane applied magnetic field $h_x = 1.1$ and an applied current density $J_{\mathrm{dc}} = 1.5 \times 10^7\ \mathrm{A\,cm^{-2}}$, where the color scale represents the different values taken by the magnetization component m_x (the vectors represent the in-plane magnetization). In this equilibrium OP configuration, the only variables different from zero, are those with $m = 1$, i.e., $a_{1j}^{\mathrm{eq}} \neq 0$. With this condition, the quantity $ae^{-i\phi} = \sum_j N_{1j} a_{1j} J_m(\chi_{1j}\rho/R)$ only depends on the variable ρ. Finally, the component $m_\phi \approx i(a^* e^{i\phi} - ae^{-i\phi})/\sqrt{2}$ is independent of the coordinate ϕ. In the absence of an applied current the configuration is completely saturated out of the plane, i.e., $a_{mj}^{\mathrm{eq}} = 0$.

B. Spin wave modes

In the following, we study the linear spin wave modes of the disk, that are dynamic magnetic excitations occurring on top of the just described equilibrium configuration, taking into account the Zeeman and Oersted fields, demagnetizing and exchange interactions, and the spin transfer torque term at a given dc current. In order to study this linear dynamics, we write $a_{mj} = a_{mj}^{\mathrm{eq}} + \tilde{a}_{mj}$, where $\tilde{a}_{mj}$ represents small dynamic deviations with respect to the equilibrium configuration. The equation of motion follows using a Taylor expansion with respect to the equilibrium magnetization:

$$i\frac{d}{d\tau}\begin{pmatrix}\tilde{a}_{mj}\\ \tilde{a}_{mj}^*\end{pmatrix} = \begin{pmatrix} A_{mj}^{m'j'} & B_{mj}^{m'j'}\\ -B_{mj}^{m'j'*} & -A_{mj}^{m'j'*}\end{pmatrix}\begin{pmatrix}\tilde{a}_{m'j'}\\ \tilde{a}_{m'j'}^*\end{pmatrix} = \mathbf{M}_{\mathrm{dc}}\begin{pmatrix}\tilde{a}_{m'j'}\\ \tilde{a}_{m'j'}^*\end{pmatrix}, \tag{46}$$

where $A_{mj}^{m'j'} = (1 - i\alpha)\partial^2\mathcal{U}_t^{\mathrm{dc}}/\partial a_{mj}^* \partial a_{m'j'}|_{\mathrm{eq}}$ and $B_{mj}^{m'j'} = (1 - i\alpha)\partial^2\mathcal{U}_t^{\mathrm{dc}}/\partial a_{mj}^* \partial a_{m'j'}^*|_{\mathrm{eq}}$. If the matrix $\mathbf{M}_{\mathrm{dc}}$ can be

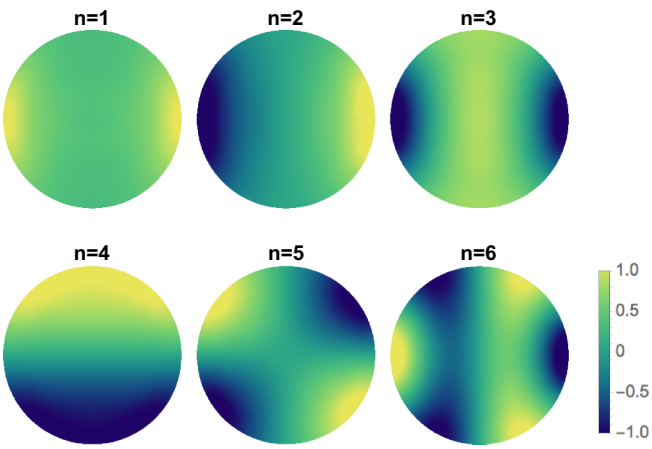

FIG. 6. Spatial form of the normal modes in the in-plane (IP) configuration, with an applied magnetic field $h_x = 0.1$. The $m_z = \sqrt{2}\mathrm{Re}(\tilde{a})$ component of the magnetization is plotted. The modes are ordered according to their frequencies: $n = 1$ with $f = 8.04$ GHz, $n = 2$ with $f = 8.48$ GHz, $n = 3$ with $f = 12.38$ GHz, $n = 4$ with $f = 12.96$ GHz, $n = 5$ with $f = 14.18$ GHz, and $n = 6$ with $f = 16.55$ GHz.

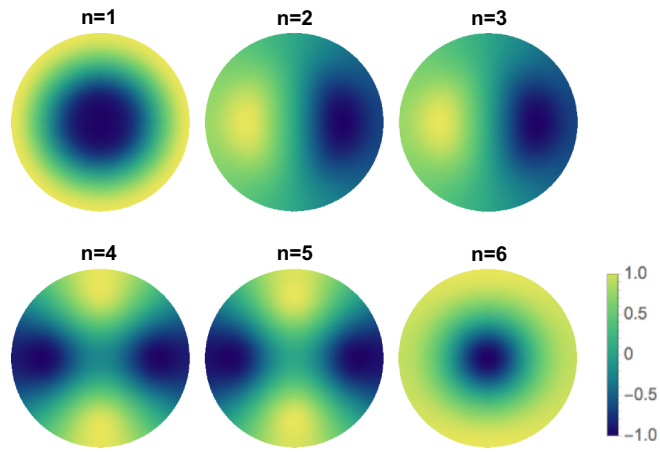

FIG. 7. Spatial form of the normal modes in the out-of-plane (OP) configuration, with an applied magnetic field $h_x = 1.1$. The $m_z = \sqrt{2}\mathrm{Re}(\tilde{a})$ component of the magnetization is plotted. The modes are ordered according to their frequencies: $n = 1$ with $f = 7.03$ GHz, $n = 2$ with $f = 9.73$ GHz, $n = 3$ with $f = 9.99$ GHz, $n = 4$ with $f = 13.15$ GHz, $n = 5$ with $f = 13.48$ GHz, and $n = 6$ with $f = 14.28$ GHz.

diagonalized, it may be written as $\mathbf{M}_{dc} = \mathbf{PDP}^{-1}$, with $\mathbf{D}$ a diagonal matrix that contains the eigenvalues of $\mathbf{M}_{\mathrm{dc}}$ and $\mathbf{P}$ has as columns the eigenvectors of the matrix $\mathbf{M}_{\mathrm{dc}}$. The variables $\tilde{a}_{mj}$ do no represent the normal mode amplitudes, thus we do the following Bogoliubov transformation that accomplishes the mentioned diagonalization:

$$\begin{pmatrix} \tilde{a}_{mj} \\ \tilde{a}^*_{mj} \end{pmatrix} = \begin{pmatrix} \lambda^n_{mj} & -\mu^n_{mj} \\ -(\mu^n_{mj})^* & (\lambda^n_{mj})^* \end{pmatrix} \begin{pmatrix} b_n \\ b^*_n \end{pmatrix} = \mathbf{P} \begin{pmatrix} b_n \\ b^*_n \end{pmatrix}. \tag{47}$$

Thus the equations for the new variables b_n and b^*_n become diagonal:

$$i\frac{d}{d\tau}\begin{pmatrix} b_n \\ b^*_n \end{pmatrix} = \mathbf{D}\begin{pmatrix} b_n \\ b^*_n \end{pmatrix} = \begin{pmatrix} \omega_n + i\gamma_n & 0 \\ 0 & -\omega_n + i\gamma_n \end{pmatrix}\begin{pmatrix} b_n \\ b^*_n \end{pmatrix}, \tag{48}$$

and their solution is directly $b_n(\tau) = b^0_n e^{(-i\omega_n+\gamma_n)\tau}$. Here the frequencies are normalized, so that $f_n = 2M_s|\gamma|\omega_n$ is the frequency in hertz. The coefficient γ_n associated with the exponential growth of this solution is negative for dc currents below the critical current density associated with auto-oscillations, i.e., in this case $b_n(\tau) \to 0$ when $\tau \to \infty$.

In Figs. 6 and 7, the component $m_z = \sqrt{2}Re(\tilde{a})$ of the magnetization is plotted for the first normal modes of oscillation, for the in-plane (IP) and out-of-plane configurations (OP) respectively, and in the absence of an applied current. In order to obtain $a(\vec{\rho},\tau)$ associated with a given mode, one needs to recall the expansion of Eq. (7), and that $\tilde{a}_{mj} = b^0_n(\lambda^n_{mj}e^{-i\omega_n\tau} - \mu^n_{mj}e^{i\omega_n\tau})$ for mode n, with b^0_n a constant that may be taken as real (there is an overall arbitrary phase associated with the initial time).

Figure 6 corresponds to an IP configuration, with $h_x = 0.1$: the modes are stationary, and have symmetry or antisymmetry properties under reflections with respect to the x axis ($\phi \to -\phi$) or with respect to the y axis ($\phi \to \pi - \phi$). Numerically, we found that there are modes with $\lambda^n_{-mj} = (-1)^m\lambda_{mj}$ and $\mu^n_{-mj} = (-1)^m\mu_{mj}$, or $\lambda^n_{-mj} = -(-1)^m\lambda_{mj}$ and $\mu^n_{-mj} = -(-1)^m\mu_{mj}$. In the first case,

$$m_z = \sqrt{2}b^0_n\left[\sum_j N_{0j}\left(\lambda^n_{0j} - \mu^n_{0j}\right)J_0(\kappa_{0j}\rho)\cos(\omega_n\tau) + 2\sum_{m>0j} N_{mj}J_m(\kappa_{mj}\rho)\left(\lambda^n_{mj} - \mu^n_{mj}\right)\cos(m\phi)\cos(\omega_n\tau)\right], \tag{49}$$

i.e., these are stationary modes with reflection symmetry with respect to the x axis (or with respect to $\phi \to -\phi$). And in the second case:

$$m_z = 2\sqrt{2}b^0_n\sum_{m>0j} N_{mj}J_m(\kappa_{mj}\rho)\left(\lambda^n_{mj} + \mu^n_{mj}\right) \times \sin(m\phi)\sin(\omega_n\tau), \tag{50}$$

i.e., these modes are stationary and antisymmetric with respect to reflections with respect to the x axis (antisymmetry with $\phi \to -\phi$). Also, the modes separate into those with m even and m odd (the second condition only arises if $\lambda^n_{0j} = 0$ and $\mu^n_{0j} = 0$), and this leads to antisymmetric or symmetric modes with respect to reflections with respect to the y axis, that depends on them being proportional to $\cos(m\phi)$ or to $\sin(m\phi)$, respectively.

Figure 7 corresponds to the out-of-plane configuration (OP), for an applied magnetic field $h_x = 1.1$. These are stationary modes in the radial direction, but in the angular direction they propagate either clockwise or anti-clockwise. The modes ($n = 2$) and ($n = 3$) are quasi-degenerate, the one with lowest frequency turns counter-clockwise, while the other clockwise [37]. The same happens with modes

($n = 4$) and ($n = 5$). Numerically, we found that the modes may be understood in the following manner. The modes may be described in an approximate way if one considers that $\lambda_{m'j'} = \delta^m_{m'}\delta^j_{j'}$ and $\mu_{m'j'} = 0$, for a given m and j for each mode. In this way,

$$m_z \approx 2\sqrt{2}b_n^0 N_{mj} J_m(\kappa_{mj}\rho)\lambda^n_{mj}\cos(\omega_n\tau - m\phi). \tag{51}$$

Thus, these are modes stationary in the radial direction, but that do rotate anticlockwise (if $m > 0$) or clockwise (if $m < 0$) with respect to the angular direction. The mode $n = 1$ is associated to $\lambda_{00} \approx 1$, the mode $n = 2$ to $\lambda_{11} \approx 1$, the mode $n = 3$ to $\lambda_{-11} \approx 1$, and then successively.

Figures 6 and 7, obtained with our analytic-numeric method, may be compared with similar ones obtained with usual micromagnetic methods. For the IP configuration the form of the modes $n = 1,2,3$ of our Fig. 6 are very similar to the modes (0,0), (1,0), and (2,0) represented in Fig. 2 of Ref. [24]. The frequencies are also similar, the small differences are due to the parameters used for permalloy. Also, for the OP configuration the modes $n = 1,2$ of our Fig. 7 also compare well to the modes (0,0) and (0,1) of Fig. 4 of Ref. [24].

C. Excitation with an alternating current

We now consider the excitation of the magnetization dynamics of the disk via an alternating current, considering the case where there is a dc current density applied but below its critical value. Thus, in this case in the absence of the alternating current, we are under the condition that the normal modes have their associated coefficient $\gamma_n < 0$, i.e., the normal modes decay in time and there is an equilibrium configuration, described in Sec. IV A. The total current density is now

$$J = J_{\rm dc} + J_{\rm ac}\cos(\Omega\tau). \tag{52}$$

The alternating current density has associated the following terms in the effective energy: $\mathcal{U}_t^{\rm ac} = \mathcal{U}_O^{\rm ac} + i\mathcal{U}_{\rm stt}^{\rm ac}$. In the presence of this alternating current density, the equations of motion for the deviations $\tilde{a}_{mj}$ from the equilibrium configuration are

$$\begin{aligned} i\frac{d}{d\tau}\begin{pmatrix}\tilde{a}_{mj}\\ \tilde{a}^*_{mj}\end{pmatrix} &= \begin{pmatrix} A^{m'j'}_{mj} & B^{m'j'}_{mj}\\ -B^{m'j'*}_{mj} & -A^{m'j'*}_{mj}\end{pmatrix}\begin{pmatrix}\tilde{a}_{m'j'}\\ \tilde{a}^*_{m'j'}\end{pmatrix}\\ &\quad + \left[\begin{pmatrix} C_{m'j'}\\ -C^*_{m'j'}\end{pmatrix} + \begin{pmatrix} D^{m'j'}_{mj} & E^{m'j'}_{mj}\\ -E^{m'j'*}_{mj} & -D^{m'j'*}_{mj}\end{pmatrix}\begin{pmatrix}\tilde{a}_{m'j'}\\ \tilde{a}^*_{m'j'}\end{pmatrix}\right]\\ &= \mathbf{M}_{\rm dc}\begin{pmatrix}\tilde{a}_{m'j'}\\ \tilde{a}^*_{m'j'}\end{pmatrix} + \left[\mathbf{V}_{\rm ac} + \mathbf{M}_{\rm ac}\begin{pmatrix}\tilde{a}_{m'j'}\\ \tilde{a}^*_{m'j'}\end{pmatrix}\right], \end{aligned} \tag{53}$$

with $C^{m'j'}_{mj} = (1 - i\alpha)\partial\mathcal{U}_t^{\rm ac}/\partial a^*_{mj}|_{\rm eq}$, $D^{m'j'}_{mj} = (1 - i\alpha)\partial^2\mathcal{U}_t^{\rm ac}/\partial a^*_{mj}\partial a_{m'j'}|_{\rm eq}$, and $E^{m'j'}_{mj} = (1 - i\alpha)\partial^2\mathcal{U}_t^{\rm ac}/\partial a^*_{mj}\partial a^*_{m'j'}|_{\rm eq}$. The same previous change of variables done to find normal modes [Eq. (47)] is used, and we obtain the following equations of motion for the amplitudes b_n and their conjugates:

$$i\frac{d}{d\tau}\begin{pmatrix}b_n\\ b^*_n\end{pmatrix} = \mathbf{P}^{-1}\mathbf{M}_{\rm dc}\mathbf{P}\begin{pmatrix}b_{n'}\\ b^*_{n'}\end{pmatrix} + \left[\mathbf{P}^{-1}\mathbf{V}_{\rm ac} + \mathbf{P}^{-1}\mathbf{M}_{\rm ac}\mathbf{P}\begin{pmatrix}b_{n'}\\ b^*_{n'}\end{pmatrix}\right], \tag{54}$$

that can be written in the following way:

$$\begin{aligned} i\frac{d}{d\tau}\begin{pmatrix}b_n\\ b^*_n\end{pmatrix} &= \begin{pmatrix}\omega_n + i\gamma_n & 0\\ 0 & -\omega_n + i\gamma_n\end{pmatrix}\begin{pmatrix}b_n\\ b^*_n\end{pmatrix} + \left[\begin{pmatrix}A_n\\ -A^*_n\end{pmatrix}\right.\\ &\quad \left. + \begin{pmatrix}B^{n'}_n & C^{n'}_n\\ -C^{n'*}_n & -B^{n'*}_n\end{pmatrix}\begin{pmatrix}b_{n'}\\ b^*_{n'}\end{pmatrix}\right] J_{\rm ac}\cos(\Omega t). \end{aligned} \tag{55}$$

1. Ferromagnetic resonance, role of the Oersted field

If one excites the system with an alternating current density with a frequency similar to the frequency ω_n of a given mode, i.e., $\Omega \sim \omega_n$, one expects a response at the same exciting frequency Ω, i.e., a solution of the form $b_n = b_n^0 e^{-i\Omega\tau}$. When considering only resonant terms, Eq. (55) leads to

$$\begin{aligned} \begin{pmatrix}\Omega & 0\\ 0 & -\Omega\end{pmatrix}\begin{pmatrix}b^0_n\\ b^{0*}_n\end{pmatrix} &= \begin{pmatrix}\omega_n + i\gamma_n & 0\\ 0 & -\omega_n + i\gamma_n\end{pmatrix}\begin{pmatrix}b^0_n\\ b^{0*}_n\end{pmatrix}\\ &\quad + \begin{pmatrix}A_n\\ -A^*_n\end{pmatrix} J_{\rm ac}/2. \end{aligned} \tag{56}$$

Thus the amplitude b_n^0 becomes

$$|b_n^0| = \frac{|A_n|J_{\rm ac}/2}{\sqrt{(\Omega - \omega_n)^2 + \gamma_n^2}}, \tag{57}$$

showing as expected a resonant response when $\Omega \simeq \omega_n$. The oscillation amplitude is maximal when $\Omega = \omega_n$, and the width of the resonance is basically $|\gamma_n|$ (notice that when $J_{\rm dc} \to J^C_{\rm dc}$, $\gamma_n \to 0$). If taking into account the Oersted field, in both the (IP) and (OP) configurations, the coefficient A_n is maximal for $n = 2$. For these modes, the maximum amplitude corresponds to a_{11}. In the absence of the Oersted field, it would be impossible to excite in a direct way the mentioned modes.

The response of the system to the alternating current, may be measured by the following quantity:

$$\sum_n |b_n^0|^2 \sim \sum_n \frac{|A_n|^2}{(\Omega - \omega_n)^2 + \gamma_n^2}. \tag{58}$$

In Fig. 8, the previous response is plotted as a function of the frequency of the alternating current in the IP configuration. If one does not consider the Oersted field, only the ($n = 5$) mode is excited (continuous orange line). Taking into account the Oersted field the lowest mode excited corresponds to the ($n = 2$) mode (dashed blue line). In Fig. 9, the response function is plotted as a function of frequency for the OP configuration. The plot considers the effect of the Oersted field, in its absence the spin wave modes are not excited. In the IP configuration, in the absence of the Oersted field, the $a^{\rm eq}_{mj} \neq 0$, but in the OP configuration the $a^{\rm eq}_{mj} = 0$ in the absence of the Oersted field. Due to this difference in the absence of the Oersted field, it is only possible to excite via the spin transfer torque the spin wave modes of the disk in the IP configuration, but not in the OP configuration.

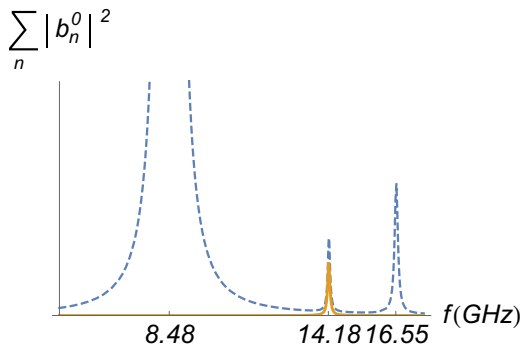

FIG. 8. Measure of the response of the system, $\sum_n |b_n^0|^2$, when there is an alternating current applied, in arbitrary units and as a function of frequency, for an IP configuration. A magnetic field $h_x = 0.1$ is applied and there is no dc current applied. The dashed blue line considers the Oersted field, the modes $(n = 2)$, $(n = 5)$, and $(n = 6)$ are excited. The continuous orange line does not consider the Oersted field, only the $(n = 5)$ mode is excited.

2. *Parametric resonance, role of the out-of-plane component of the spin transfer torque*

If one excites the system with a frequency that is approximately twice the frequency of a given normal mode, i.e., $\Omega \sim 2\omega_n$, we expect the response to be at a frequency that is approximately at half the value of the frequency Ω, i.e., we search for a solution of the form $b_n = b_n^0 e^{(-i\Omega/2+\Gamma)\tau}$. Considering only resonant terms, we find that Eq. (55) leads to

$$\begin{pmatrix} \left(\frac{\Omega}{2} - \omega_n\right) + i(\Gamma - \gamma_n) & C_n J_{\rm ac}/2 \\ -C_n^* J_{\rm ac}/2 & \left(\omega_n - \frac{\Omega}{2}\right) + i(\Gamma - \gamma_n) \end{pmatrix} \begin{pmatrix} b_n^0 \\ b_n^{0*} \end{pmatrix} = 0. \tag{59}$$

A nonzero solution of Eq. (59) is obtained by imposing the associated determinant to be null, i.e.,

$$(\Gamma - \gamma_n) = \sqrt{J_{\rm ac}^2 |C_n|^2/4 - (\Omega/2 - \omega_n)^2}. \tag{60}$$

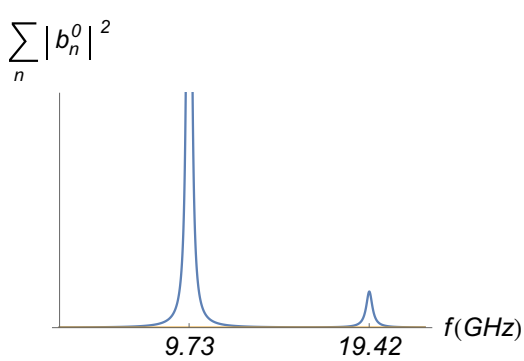

FIG. 9. Measure of the response of the system, $\sum_n |b_n^0|^2$, when there is an alternating current applied, in arbitrary units and as a function of frequency for an OP configuration. A magnetic field $h_x = 1.1$ is applied and there is no dc current applied. The excitation is via the Oersted field, the lowest mode excited corresponds to the $(n = 2)$ mode.

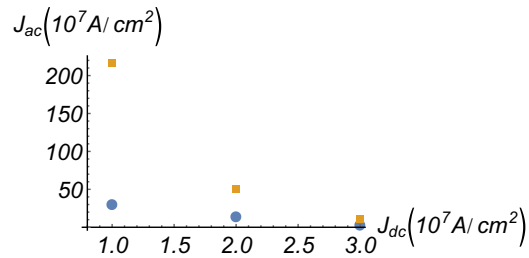

FIG. 10. Critical alternating current density for mode $(n = 1)$, as a function of the dc current density, for $h_x = 0.1$, IP configuration. The orange squares represent the case $\beta_\perp = 0$, while the blue points $\beta_\perp = 0.1\beta_{||}$.

In order for the amplitude b_n of mode (n) to start growing exponentially, it must happen that $\Gamma > 0$. Thus the critical ac current density for the development of auto-oscillations is given by $\Gamma = 0$, i.e.,

$$J_{\rm ac}^C = 2\sqrt{\gamma_n^2 + (\Omega/2 - \omega_n)^2}/|C_n|. \tag{61}$$

Thus, the ac critical current density is minimal when $\Omega/2 = \omega_n$, furthermore, it has an associated width as a function of frequency Ω equal to $2|\gamma_n|$, and it depends also on the absolute value of the coefficient C_n.

In the IP configuration the coefficient C_n is highly sensible to the variation of the parameter $\beta_\perp$. It is possible to excite parametrically all the normal modes of oscillation, and the spin transfer torque plays an important role in all of them. In Fig. 10, we plot the critical ac current density for the mode $(n = 1)$ as a function of the dc current density applied (we take $\Omega/2 = \omega_n$, and the applied magnetic field is $h_x = 0.1$). It is seen that the value of the ac critical current is much greater than the dc critical current in this geometry, but it is also seen that there is a large sensibility of the ac critical current to the value of the out-of-plane spin transfer torque parameter $\beta_\perp$ (the orange squares represent the case $\beta_\perp = 0$, while the blue points $\beta_\perp = 0.1\beta_{||}$). Thus a large value of $\beta_\perp$ may bring the ac critical current density to the range of the dc critical current density, meaning that a parametric resonance experiment in this system becomes a good test to determine the strength of $\beta_\perp$ versus $\beta_{||}$.

In the OP configuration, the mode $(n = 1)$ corresponds to the quasiuniform mode and it cannot be excited parametrically, and coincides with the conclusions of our macro-spin analysis. The first mode that may be excited parametrically is the $(n = 2)$ mode, where the out-of-plane spin transfer torque plays an important role. In Fig. 11, the critical ac current density is plotted for the mode $(n = 2)$ as a function of the dc current density applied, with $h_x = 1.1$.

Our results may be used to explain the results of Ref. [29]. They compare their experiments and their macro-spin approximation magnetization simulations. Their results present a qualitative accord, there are quantitative discrepancies. We think these discrepancies may be explained if a perpendicular spin transfer torque term is considered. Also, using our model, the parameter $\beta_\perp$ may be estimated by comparing our numerical results with experimental measurements, as those of Fig. 2 of Ref. [28] or Fig. 3 of Ref. [30].

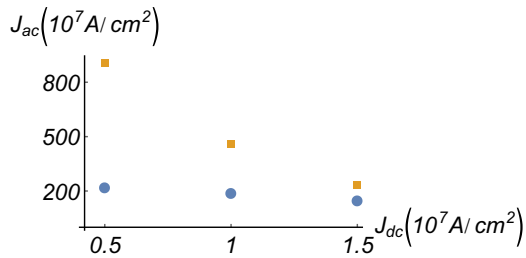

FIG. 11. Critical ac current density for the mode ($n = 2$), as a function of the dc current density, with $h_x = 1.1$, OP configuration. The orange squares represent the case $\beta_\perp = 0$, while the blue points $\beta_\perp = 0.1\beta_{||}$.

D. Excitation of spin wave normal modes with an alternating magnetic field

Here we present results on the excitation of spin wave normal modes when applying a uniform ac magnetic field in the plane of the disk in the IP configuration. The magnetic field is perpendicular to the direction of the equilibrium magnetization, i.e., in direction $\hat{y}$. This study allowed us to validate our model, since our results compare well to the micromagnetic simulations of Ref. [31]. We considered a disk with the parameters of this reference, i.e., a permalloy disk with radius $R = 250$ nm and thickness $L = 25$ nm. We studied the response as a function of applied dc magnetic field H_x, when there is an ac uniform component of the magnetic field given by $\tilde{h}_y = h_{\rm ap}\cos(\Omega\tau)$, at a fixed frequency of 10 GHz. In Fig. 12, it is observed that only a few modes are excited, specifically those which are symmetric with respect to the x axis. Of the four modes that are excited, three of them correspond to localized modes in the edges of the disk. The mode with the highest peak corresponds to the quasi-uniform mode, whose amplitude of oscillation extends to practically all the disk. The comparison of our results with the micromagnetic simulations of Ref. [31] is satisfactory, specially in terms of the modes that are excited. However, we observe quantitative differences for the resonant magnetic fields of the edge modes. The latter may be explained, since the larger the radius of the disk, in order to get higher accuracy, one needs a larger basis of functions within our model; at low radii, the exchange interaction is dominant and the spatial variation of the modes is smoother.

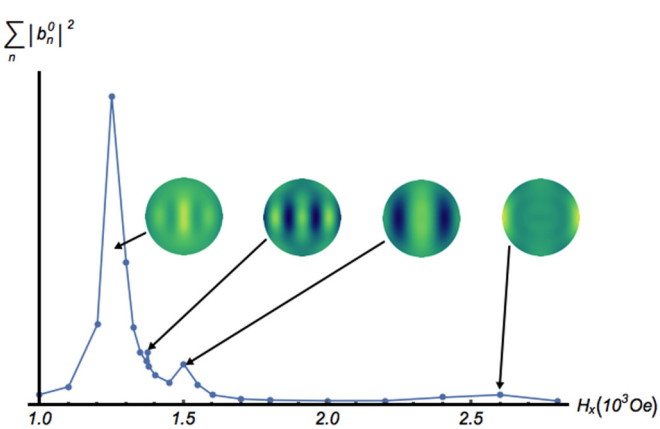

FIG. 12. Response of the normal modes of the disk as a function of dc applied magnetic field, when the spin wave modes are excited via a uniform ac magnetic field applied in plane normally to the equilibrium magnetization, at a fixed frequency of 10 GHz in Permalloy (IP configuration).

V. CONCLUSIONS AND REMARKS

We have presented the linear spin wave modes of a thin disk made of a soft ferromagnetic material, calculated in a very thin film limit approximation and also considering the full effect of the magnetostatic interaction, i.e., with edge effects included. The configurations considered are an in-plane magnetized case (IP) and an out-of-plane one (OP). We studied the excitation of these normal modes via a spin polarised electric current, with dc and ac components, considering the spin transfer torque and Oersted fields associated. We also considered excitation of the modes via alternating magnetic fields, and we did find agreement with micromagnetic simulations.

Within the simple very thin film limit approximation, in both configurations it is not possible to excite the uniform mode in a direct way, i.e., with an exciting frequency that is resonant with the frequency of the mode. It is only possible to excite the uniform mode parametrically and in the IP configuration. However, in the latter case, the ac current density needed to attain auto-oscillations (if the dc part is below its corresponding critical value) is too large to be detected experimentally, although if there is an appreciable out-of-plane component of the spin transfer torque this ac critical current diminishes significantly.

Within the model that includes the full demagnetizing field, that has associated nonequilibrium magnetization configurations, it is possible to excite the spin wave normal modes either directly or parametrically. For the case of direct excitation, the role of the Oersted field is important in both configurations: there are modes that are excited that in its absence would be "silent." Using parametric excitation the ac currents needed to attain auto-oscillations are too large, but if the out-of-plane component of the spin transfer torque is significant one may get to a point where the ac and dc critical current densities are comparable.

As a summary, the main conclusions on excitation of spin wave normal modes of a disk with ac currents, is that with exciting frequencies resonant with the frequencies of the modes (direct excitation) the role played by the Oersted field is significant, and if the exciting frequencies are twice the frequencies of the modes (parametric excitation) one sees a significant effect only for large out-of-plane components of the spin transfer torque. The latter means that parametric excitation in this geometry should be a way to distinguish experimentally a significant out-of-plane component of the spin transfer torque.

ACKNOWLEDGMENTS

D.M-A. acknowledges financial support from CONICYT by Beca Doctorado Nacional 2012, folio 21120160. D.M-A. and R.E.A acknowledge financial support from project Fondecyt 1130192 and Center for the Development of Nanoscience and Nanotechnology CEDENNA FB0807 (Chile).

APPENDIX A: OERSTED FIELD FREE ENERGY

1. In-plane configuration (IP), higher order contributions

The higher order terms of the Oersted free energy in the IP configuration are

$$\mathcal{U}_O^2 = iVh_O\left(a_{m_1j_1}a^*_{m_2j_2} - c.c\right)\delta^{m_1+1}_{m_2} i^O_{m_1j_1m_2j_2}, \tag{A1a}$$

$$\mathcal{U}_O^3 = iV\frac{h_O}{4\sqrt{2}}\left[\left[(-1)^{m_1}a^*_{-m_1j_1} - a_{m_1j_1}\right]a_{m_2j_2}a^*_{m_3j_3} - \text{c.c.}\right] \times \delta^{m_1+m_2}_{m_3-1} i^O_{m_1j_1m_2j_2m_3j_3}, \tag{A1b}$$

with the following definitions, that involve integrals that are calculated numerically:

$$i^O_{m_1j_1m_2j_2} \equiv N_{m_1j_1}N_{m_2j_2}\int_0^1 J_{m_1}\left(\chi_{m_1j_1}x\right)J_{m_2}\left(\chi_{m_2j_2}x\right)x^2dx, \tag{A2a}$$

$$i^O_{m_1j_1m_2j_2m_3j_3} \equiv N_{m_1j_1}N_{m_2j_2}N_{m_3j_3}\int_0^1 J_{m_1}\left(\chi_{m_1j_1}x\right) \times J_{m_2}\left(\chi_{m_2j_2}x\right)J_{m_3}\left(\chi_{m_3j_3}x\right)x^2dx. \tag{A2b}$$

2. Out-of-plane configuration (OP), higher-order contribution

In the OP configuration a third-order contribution to the free energy due to the Oersted field corresponds to

$$\mathcal{U}_O^{(3)} = -iV\frac{h_O}{2\sqrt{2}}\left(a_{m_1j_1}a_{m_2j_2}a^*_{m_3j_3} - a^*_{m_1j_1}a^*_{m_2j_2}a_{m_3j_3}\right) \times \delta^{m_1+m_2-m_3}_1 i^O_{m_1j_1m_2j_2m_3j_3}. \tag{A3}$$

APPENDIX B: EXCHANGE ENERGY, FOURTH-ORDER TERMS

The fourth-order term of the exchange energy is given by

$$\mathcal{U}_E^4 = \frac{h_E}{4}\int[(\vec{\nabla}a)^2a^{*2} + \text{c.c.}]R^2dV. \tag{B1}$$

In order to handle these terms, we use the following operators and results:

$$L_\pm = \frac{\partial}{\partial x} \pm i\frac{\partial}{\partial y} \Rightarrow \vec{\nabla}a\cdot\vec{\nabla}a = L_+aL_-a, \tag{B2}$$

$$L_\pm = e^{\pm i\phi}\left(\frac{\partial}{\partial\rho} \pm i\frac{1}{\rho}\frac{\partial}{\partial\phi}\right)$$

$$\Rightarrow\ L_\pm(J_m(k\rho)e^{im\phi}) = \mp kJ_{m\pm1}(k\rho)e^{i(m\pm1)\phi}. \tag{B3}$$

We integrate in ϕ, and in z, we do the change of variables $x \to \rho/R$, and it leads to

$$\mathcal{U}_E^4 = -V\frac{h_E}{2}\left(a_{m_1j_1}a_{m_2j_2}a^*_{m_3j_3}a^*_{m_4j_4} + \text{c.c.}\right) \times \delta^{m_1+m_2}_{m_3+m_4} i^E_{m_1j_1m_2j_2m_3j_3m_4j_4}, \tag{B4}$$

where we defined

$$i^E_{m_1j_1m_2j_2m_3j_3m_4j_4} \equiv \chi_{m_1j_1}\chi_{m_2j_2}N_{m_1j_1}N_{m_2j_2}N_{m_3j_3}N_{m_4j_4} \times \int_0^1 dx\,x\,J_{m_1+1}\left(\chi_{m_1j_1}x\right)J_{m_2-1}\left(\chi_{m_2j_2}x\right) \times J_{m_3}\left(\chi_{m_3j_3}x\right)J_{m_4}\left(\chi_{m_4j_4}x\right). \tag{B5}$$

APPENDIX C: DEMAGNETIZING FIELD AND DEMAGNETIZING ENERGY

To determine the demagnetizing field of our thin disk (the magnetization is assumed uniform over the thickness of the disk) we first calculate the magnetostatic potential ($\vec{H}_D = -\vec{\nabla}\Phi$), which has contributions from surface and volume effective magnetic charges:

$$\Phi(\vec{x}) = \int dS'\frac{\hat{n}\cdot\vec{M}(\vec{x}')}{|\vec{x}-\vec{x}'|} - \int dV'\frac{\vec{\nabla}\cdot\vec{M}(\vec{x}')}{|\vec{x}-\vec{x}'|}. \tag{C1}$$

$\sigma_M = (\hat{n}\cdot\vec{M})$ represents the surface magnetic charge density, with contributions from the top and bottom surfaces of the disk and from its mantle; and $\rho_M = -(\vec{\nabla}\cdot\vec{M})$ the volumetric magnetic charge density, with contributions from the interior of the disk. In order to calculate these potentials we use the following representation of the Green's function in terms of cylindrical coordinates:

$$\frac{1}{|\vec{x}-\vec{x}'|} = \sum_{m=-\infty}^{\infty} e^{im(\phi-\phi')}\int_0^\infty dk\,J_m(k\rho)J_m(k\rho')e^{-k|z-z'|}. \tag{C2}$$

The demagnetizing field averaged over the thickness of the disk can be separated into two parts:

(a) Its component in the perpendicular direction to the plane, with contribution only from surface charges in the top and bottom surfaces:

$$\vec{H}_D^\perp = -4\pi\vec{M}_\perp(\rho,\phi) + \frac{2M_s}{L}\int_0^\infty dk f(kL) \times \sum_{m=-\infty}^{\infty}\left[\int dS'J_m(k\rho')\vec{m}_\perp(\rho',\phi')e^{-im\phi'}\right]J_m(k\rho)e^{im\phi}, \tag{C3}$$

with $f(u) \equiv \exp(-u) - 1 + u$.

(b) Its in-plane components, with contributions from mantle surface charges as well as volume charges:

$$\vec{H}_D^{||} = -\frac{2M_s}{L}\int_0^\infty dk\frac{f(kL)}{k^2} \times \sum_{m=-\infty}^{\infty}\left[\int dS'\vec{\nabla}(J_m(k\rho')e^{-im\phi'})\cdot\vec{m}_{||}(\rho',\phi')\right] \times \vec{\nabla}(J_m(k\rho)e^{im\phi}). \tag{C4}$$

Furthermore, the demagnetizing energy is calculated in the following form:

$$\mathcal{U}_D = -\frac{1}{8\pi M_s^2}\int[\vec{H}_D^\perp + \vec{H}_D^{||}]\cdot\vec{M}dV. \tag{C5}$$

We write the magnetization components in the following way: ($M_\pm \equiv M_x \pm iM_y$ and $M_\pm \equiv M_z \pm iM_y$ in the configurations in which the disk is magnetized in plane and out of plane, respectively):

$$M_\perp = M_s\sum_{lj}\sigma_{lj}N_{lj}J_l(\kappa_{lj}\rho)e^{il\phi},$$

$$M_\pm = M_s\sum_{lj}\sigma^\pm_{lj}N_{lj}J_l(\kappa_{lj}\rho)e^{il\phi}. \tag{C6}$$

Using Eqs. (C3)–(C6), one obtains the demagnetizing energy as follows, $\mathcal{U}_D = \mathcal{U}_D^{\perp} + \mathcal{U}_D^{\parallel}$, with

$$\mathcal{U}_D^{\perp} = \frac{1}{2}\sum_{l_1 j_1 j_2}(-1)^{l_1}\sigma_{l_1 j_1}^{\perp}\sigma_{-l_1 j_2}^{\perp}\left(\delta_{j_2}^{j_1} - 2V I_{(l_1,j_1,j_2,L/R)}^{1}\right), \quad \text{(C7a)}$$

$$\mathcal{U}_D^{\parallel} = -\frac{V}{4}\sum_{l_1 j_1 j_2}(-1)^{l_1}\left(\sigma_{l_1 j_1}^{-}\sigma_{(-l_1-2)j_2}^{-} I_{(l_1,j_1,j_2,L/R)}^{2} + \sigma_{l_1 j_1}^{+}\sigma_{(-l_1+2)j_2}^{+} I_{(l_1,j_1,j_2,L/R)}^{3} - 2\sigma_{l_1 j_1}^{+}\sigma_{(-l_1)j_2}^{-} I_{(l_1,j_1,j_2,L/R)}^{1}\right), \quad \text{(C7b)}$$

where the $\sigma_{lj}^{\perp}, \sigma_{lj}^{+}$ y σ_{lj}^{-} are functions of the variables a_{mj} [see Eqs. (5) and (7)], with details of these expressions in Appendixes C 1 and C 2; and the $I_{(l_1,j_1,j_2,L/R)}^{1}$, $I_{(l_1,j_1,j_2,L/R)}^{2}$, $I_{(l_1,j_1,j_2,L/R)}^{3}$ represent integrals that are calculated numerically, with details in Appendix C 3.

1. Configuration magnetized in plane

In the in-plane configuration (IP), we have that

$$M_{\perp} = M_z = (a + a^*)\sqrt{2 - aa^*}/2, \quad \text{(C8a)}$$

$$M_{\pm} = M_x \pm i M_y = (1 - aa^*) \pm (a - a^*)\sqrt{2 - aa^*}/2. \quad \text{(C8b)}$$

The $\sigma_{lj}'s$ [defined through Eq. (C6)] are functions of the $a_{mj}'s$ [defined through Eqs. (5) and (7)]. These may be expanded in power series of the $a_{mj}'s$ as follows (superindices indicate the order of approximation):

$$\sigma_{lj}^{\perp(0)} = 0 = \sigma_{lj}^{\perp(2)} = \sigma_{lj}^{\perp(4)}, \quad \text{(C9a)}$$

$$\sigma_{lj}^{\perp(1)} = (a_{lj} + (-1)^l a_{-lj}^*)/\sqrt{2}, \quad \text{(C9b)}$$

$$\sigma_{lj}^{\perp(3)} = -\frac{V}{2\sqrt{2}}\sum_{m_1 j_1 m_2 j_2 m_3 j_3}\left(a_{m_1 j_1} + (-1)^{m_1} a_{-m_1 j_1}^*\right) \times a_{m_2 j_2} a_{m_3 j_3}^* i_{dljm_1 j_1 m_2 j_2 m_3 j_3}^{4}\delta_l^{m_1+m_2-m_3}, \quad \text{(C9c)}$$

$$\sigma_{00}^{z\,(0)} = \sigma_{00}^{+(0)} = \sigma_{00}^{-(0)} = \sqrt{V}, \quad \text{(C9d)}$$

$$\sigma_{lj}^{+(1)} = -\sigma_{lj}^{-(1)} = (a_{lj} - (-1)^l a_{-lj}^*)/\sqrt{2}, \quad \text{(C9e)}$$

$$\sigma_{lj}^{+(2)} = \sigma_{lj}^{-(2)} = -2\sum_{m_1 j_1 m_2 j_2} a_{m_1 j_1} a_{m_2 j_2}^* \delta_l^{m_1-m_2} i_{d(ljm_1 j_1 m_2 j_2)}^{3}, \quad \text{(C9f)}$$

$$\sigma_{lj}^{+(3)} = -\sigma_{lj}^{-(3)} = \sigma_{lj}^{z\,(3)}, \quad \text{(C9g)}$$

$$\sigma_{lj}^{+(4)} = \sigma_{lj}^{-(4)} = 0 \quad \text{(C9h)}$$

with $i_{d(ljm_1 j_1 m_2 j_2)}^{3}$ and $i_{d(ljm_1 j_1 m_2 j_2)}^{4}$ integrals defined in Appendix C 3.

2. Configuration magnetized out of plane

In the out-of-plane configuration (OP), we have that

$$M_{\perp} = M_x = 1 - aa^*, \quad \text{(C10a)}$$

$$M_{\pm} = M_z \pm i M_y = [(a + a^*) \pm (a - a^*)]\sqrt{2 - aa^*}/2. \quad \text{(C10b)}$$

The $\sigma_{lj}'s$ [defined through Eq. (C6)] are functions of the $a_{mj}'s$ [defined through Eqs. (5) and (7)]. These may be expanded in power series of the $a_{mj}'s$ as follows (superindices indicate the order of approximation):

$$\sigma_{lj}^{\perp(1)} = 0 = \sigma_{lj}^{\perp(3)} = \sigma_{lj}^{\perp(4)}, \quad \text{(C11a)}$$

$$\sigma_{00}^{\perp(0)} = \sqrt{V}, \quad \text{(C11b)}$$

$$\sigma_{lj}^{\perp(2)} = -2V\sum_{m_1 l_1 m_2 l_2} a_{m_1 l_1} a_{m_2 l_2}^* \delta_l^{m_1-m_2} i_{d(ljm_1 l_1 m_2 l_2)}^{3}, \quad \text{(C11c)}$$

$$\sigma_{-l'j'}^{-1} = \sqrt{2}(-1)^{l'} a_{l'j'}^* = (-1)^{l'}\left(\sigma_{l'j'}^{+1}\right)^*, \quad \text{(C11d)}$$

$$\sigma_{-l'j'}^{-3} = -V\frac{1}{2\sqrt{2}}\sum_{m_1 j_1 m_2 j_2 m_3 j_3}(-1)^{l'} a_{m_1 j_1}^* a_{m_3 j_3} a_{m_2 j_2}^* \times i_{d(l'j'm_1 j_1 m_2 j_2 m_3 j_3)}^{4}\delta_{l'}^{m_1+m_2-m_3} = (-1)^{l'}\left(\sigma_{l'j'}^{+3}\right)^* \quad \text{(C11e)}$$

$$\sigma_{lj}^{\pm(0)} = \sigma_{lj}^{\pm(2)} = \sigma_{lj}^{\pm(4)} = 0 \quad \text{(C11f)}$$

with $i_{d(ljm_1 j_1 m_2 j_2)}^{3}$ and $i_{d(ljm_1 j_1 m_2 j_2)}^{4}$ integrals defined in Appendix C 3.

3. Integrals calculated numerically

Integrals calculated numerically are

$$I_{(l_1,j_1,j_2,L/R)}^{1} = N_{l_1 j_1} N_{l_1 j_2} J_{l_1}\left(\chi_{j_1}^{l_1}\right) J_{l_1}\left(\chi_{j_2}^{l_1}\right) \times \int_0^{\infty} dk \frac{f(kL/R)k^2 J_{l_1}'(k)^2}{(L/R)\left(k^2 - \left(\chi_{j_1}^{l_1}\right)^2\right)\left(k^2 - \left(\chi_{j_2}^{l_1}\right)^2\right)}, \quad \text{(C12a)}$$

$$I_{(l_1,j_1,j_2,L/R)}^{2} = N_{l_1 j_1} N_{(l_1+2)j_2} J_{l_1}(\chi_{j_1}^{l_1}) J_{l_1+2}\left(\chi_{j_2}^{l_1+2}\right) \times \int_0^{\infty} dk \frac{f(kL/R)k^2 J_{l_1}'(k) J_{l_1+2}'(k)}{(L/R)\left(k^2 - (\chi_{j_1}^{l_1})^2\right)\left(k^2 - \left(\chi_{j_2}^{l_1+2}\right)^2\right)}, \quad \text{(C12b)}$$

$$I_{(l_1,j_1,j_2,L/R)}^{3} = N_{l_1 j_1} N_{(l_1-2)j_2} J_{l_1}\left(\chi_{j_1}^{l_1}\right) J_{l_1-2}\left(\chi_{j_2}^{l_1-2}\right) \times \int_0^{\infty} dk \frac{f(kL/R)k^2 J_{l_1}'(k) J_{l_1-2}'(k)}{(L/R)\left(k^2 - \left(\chi_{j_1}^{l_1}\right)^2\right)\left(k^2 - \left(\chi_{j_2}^{l_1-2}\right)^2\right)}. \quad \text{(C12c)}$$

$$i_{d(ljm_1 j_1 m_2 j_2)}^{3} = N_{lj} N_{m_1 j_1} N_{m_2 j_2}\int_0^1 J_l\left(\chi_j^l x\right) J_{m_1}\left(\chi_{j_1}^{m_1} x\right) \times J_{m_2}\left(\chi_{j_2}^{m_2} x\right) x dx, \quad \text{(C13a)}$$

$$i_{d(ljm_1 j_1 m_2 j_2 m_3 j_3)}^{4} = N_{lj} N_{m_1 j_1} N_{m_2 j_2} N_{m_3 j_3}\int_0^1 J_l\left(\chi_j^l x\right) J_{m_1} \times \left(\chi_{j_1}^{m_1} x\right) J_{m_2}\left(\chi_{j_2}^{m_2} x\right) J_{m_3}\left(\chi_{j_3}^{m_3} x\right) x dx. \quad \text{(C13b)}$$

APPENDIX D: SPIN TRANSFER TORQUE, FOURTH-ORDER TERMS

The fourth-order terms of the spin transfer torque effective energy are

$$\mathcal{U}_{stt}^{(4)} = -\frac{\beta_{||} J V}{2} a_{m_1 j_1} a^*_{m_2 j_2} a_{m_3 j_3} a^*_{m_4 j_4} i^4_{d(m_1 j_1 m_2 j_2 m_3 j_3 m_4 j_4)} \delta^{m_1+m_3}_{m_2+m_4}. \tag{D1}$$

[1] J. C. Slonczewski, Current-driven excitation of magnetic multilayers, J. Magn. Magn. Mater. **159**, L1 (1996).

[2] L. Berger, Emission of spin waves by a magnetic multilayer traversed by a current, Phys. Rev. B **54**, 9353 (1996).

[3] I. Žutić, J. Fabian, and S. Das Sarma, Spintronics: Fundamentals and applications, Rev. Mod. Phys. **76**, 323 (2004).

[4] S. A. Wolf, D. D. Awschalom, R. A. Buhrman, J. M. Daughton, S. von Molnár, M. L. Roukes, A. Y. Chtchelkanova, and D. M. Treger, Spintronics: A spin-based electronics vision for the future, Science **294**, 1488 (2001).

[5] A. Fert, Nobel Lecture: Origin, development, and future of spintronics, Rev. Mod. Phys. **80**, 1517 (2008).

[6] S. Neusser and D. Grundler, Magnonics: Spin waves on the nanoscale, Adv. Mater. **21**, 2927 (2009).

[7] B. Lenk, H. Ulrichs, F. Garbs, and M. Münzenberg, The building blocks of magnonics, Phys. Rep. **507**, 107 (2011).

[8] S. O. Demokritov and A. N. Slavin, *Magnonics: From Fundamentals to Applications* (Springer-Verlag, Berlin, Heidelberg, 2013).

[9] V. V. Kruglyak, S. O. Demokritov, and D. Grundler, Magnonics, J. Phys. D **43**, 264001 (2010).

[10] Z. Zeng, G. Finocchio, and H. Jiang, Spin transfer nano-oscillators, Nanoscale **5**, 2219 (2013).

[11] A. D. Kent, A nanomagnet oscillator, Nat. Mater. **6**, 399 (2007).

[12] S. E. Russek, W. H. Rippard, T. Cecil, and R. Heindl, *Handbook of Nanophysics: Functional Nanomaterial* (CRC Press, Boca Raton, 2010), Chap. 38.

[13] S. I. Kiselev, J. C. Sankey, I. N. Krivorotov, N. C. Emley, A. G. F. Garcia, R. A. Buhrman, and D. C. Ralph, Spin-transfer excitations of permalloy nanopillars for large applied currents, Phys. Rev. B **72**, 064430 (2005).

[14] D. C. Ralph and M. D. Stiles, Spin transfer torques, J. Magn. Magn. Mater. **320**, 1190 (2008).

[15] D. Mancilla-Almonacid and R. E. Arias, Instabilities of spin torque driven auto-oscillations of a ferromagnetic disk magnetized in plane, Phys. Rev. B **93**, 224416 (2016).

[16] E. Schlomann and J. J. Green, Ferromagnetic Resonance at High Power Levels, Phys. Rev. Lett. **3**, 129 (1959).

[17] V. S. L'vov, *Wave Turbulence Under Parametric Excitation* (Springer-Verlag, Berlin, 1994).

[18] P. Krivosik and C. E. Patton, Hamiltonian formulation of nonlinear spin-wave dynamics: Theory and applications, Phys. Rev. B **82**, 184428 (2010).

[19] S. M. Rezende, F. M. de Aguiar, and A. Azevedo, Spin-Wave Theory for the Dynamics Induced by Direct Currents in Magnetic Multilayers, Phys. Rev. Lett. **94**, 037202 (2005).

[20] A. N. Slavin and P. Kabos, Approximate theory of microwave generation in a current-driven magnetic nanocontact magnetized in an arbitrary direction, IEEE Trans. Magn. **41**, 1264 (2005).

[21] R. E. Arias and D. L. Mills, Theory of ferromagnetic resonance in perpendicularly magnetized nanodisks: Excitation by the Oersted field, Phys. Rev. B **79**, 144404 (2009).

[22] V. V. Naletov, G. de Loubens, G. Albuquerque, S. Borlenghi, V. Cros, G. Faini, J. Grollier, H. Hurdequint, N. Locatelli, B. Pigeau, A. N. Slavin, V. S. Tiberkevich, C. Ulysse, T. Valet, and O. Klein, Identification and selection rules of the spin-wave eigenmodes in a normally magnetized nanopillar, Phys. Rev. B **84**, 224423 (2011).

[23] A. Hamadeh, G. de Loubens, V. V. Naletov, J. Grollier, C. Ulysse, V. Cros, and O. Klein, Autonomous and forced dynamics in a spin-transfer nano-oscillator: Quantitative magnetic-resonance force microscopy, Phys. Rev. B **85**, 140408(R) (2012).

[24] M. Pauselli and G. Carlotti, Spin wave eigenmodes excited by spin transfer torque in circular nanopillars: Influence of lateral size and Oersted field studied by micromagnetic simulations, J. Phys. D: Appl. Phys. **48**, 415001 (2015).

[25] M. G. Clerc, S. Coulibaly, D. Laroze, A. O. León, and A. S. Núñez, Alternating spin-polarized current induces parametric resonance in spin valves, Phys. Rev. B **91**, 224426 (2015).

[26] S. Urazhdin, V. Tiberkevich, and A. Slavin, Parametric Excitation of a Magnetic Nanocontact by a Microwave Field, Phys. Rev. Lett. **105**, 237204 (2010).

[27] F. Guo, L. M. Belova, and R. D. McMichael, Parametric pumping of precession modes in ferromagnetic nanodisks, Phys. Rev. B **89**, 104422 (2014).

[28] E. R. J. Edwards, H. Ulrichs, V. E. Demidov, S. O. Demokritov, and S. Urazhdin, Parametric excitation of magnetization oscillations controlled by pure spin current, Phys. Rev. B **86**, 134420 (2012).

[29] C. Wang, H. Seinige, and M. Tsoi, Current-driven parametric resonance in magnetic multilayers, J. Phys. D: Appl. Phys. **46**, 285001 (2013).

[30] P. Durrenfeld, E. Iacocca, J. Akerman, and P. K. Muduli, Parametric excitation in a magnetic tunnel junction-based spin torque oscillator, Appl. Phys. Lett. **104**, 052410 (2014).

[31] F. Guo, L. M. Belova, and R. D. McMichael, Spectroscopy and Imaging of Edge Modes in Permalloy Nanodisks, Phys. Rev. Lett. **110**, 017601 (2013).

[32] A. A. Timopheev, R. Sousa, M. Chshiev, L. D. Buda-Prejbeanu, and B. Dieny, Respective influence of in-plane and out-of-plane spin-transfer torques in magnetization switching of perpendicular magnetic tunnel junctions, Phys. Rev. B **92**, 104430 (2015).

[33] J. C. Sankey, Y.-T. Cui, J. Z. Sun, J. C. Slonczewski, R. A. Buhrman, and D. C. Ralph, Measurement of the spin-transfer-torque vector in magnetic tunnel junctions, Nat. Phys. **4**, 67 (2008).

[34] S. Zhang, P. M. Levy, and A. Fert, Mechanisms of Spin-Polarized Current-Driven Magnetization Switching, Phys. Rev. Lett. **88**, 236601 (2002).

[35] K. Yu. Guslienko, S. O. Demokritov, B. Hillebrands, and A. N. Slavin, Effective dipolar boundary conditions for dynamic magnetization in thin magnetic stripes, Phys. Rev. B **66**, 132402 (2002).

[36] K. Yu. Guslienko and A. N. Slavin, Boundary conditions for magnetization in magnetic nanoelements, Phys. Rev. B **72**, 014463 (2005).

[37] F. Hoffmann, G. Woltersdorf, K. Perzlmaier, A. N. Slavin, V. S. Tiberkevich, A. Bischof, D. Weiss, and C. H. Back, Mode degeneracy due to vortex core removal in magnetic disks, Phys. Rev. B **76**, 014416 (2007).